

# **Towards a Theory of Tropical/Midlatitude Mass Exchange from the Earth's Surface Through the Stratosphere**

UARS Guest Investigator Program – Final Report

PI: Dana Hartley at Georgia Tech

Grant Number: NAG 5 - 2789

Period covered: 12/1/94 - 11/30/98

IN-45

011377

## **Introduction**

The main findings of this research project have been the following

- 1) There is a significant feedback from the stratosphere on tropospheric dynamics. (Hartley, Villarin, Black and Davis, *Nature*, 1998).
- 2) A detailed analysis of the interaction between tropical and polar wave breaking in controlling stratospheric mixing. (Villarin, Hartley and Black, *J. Atmos. Sci.*, 1999)

Copies of each of these papers are attached to this report. Abstracts are given below.

## **1. A New Perspective on the Dynamical Link Between the Stratosphere and Troposphere.**

Atmospheric processes of tropospheric origin can perturb the stratosphere, but direct feedback in the opposite direction is usually assumed to be negligible, despite the troposphere's sensitivity to changes in the release of wave activity into the stratosphere. Here, however, we present evidence that such a feedback exists and can be significant. We find that if the wintertime Arctic polar stratospheric vortex is distorted, either by waves propagating upward from the troposphere or by eastward-travelling stratospheric waves, then there is a concomitant redistribution of stratospheric potential vorticity that induces perturbations in key meteorological fields in the upper troposphere. The feedback is large despite the much greater mass of the troposphere: it can account for up to half of the geopotential height anomaly at the tropopause. Although the relative strength of the feedback is partly due to a cancellation between contributions to these anomalies from lower altitudes, our results imply that stratospheric dynamics and its feedback on the troposphere are more significant for climate modelling and data assimilation than was previously assumed.

## **2. Diagnosing the Polar Excitation of Subtropical Waves in the Stratosphere.**

The poleward migration of planetary scale tongues of subtropical air has often been associated with intense polar vortex disturbances in the stratosphere. This question of vortex influence is reexamined from a potential vorticity (PV) perspective. Anomalous geopotential height and wind fields associated solely with vortex PV anomalies are derived and their impact on the stratospheric subtropical circulation is evaluated. Combined PV inversion and Contour Advection (CA) calculations indicate that transient large scale disturbances of the polar vortex do have a far reaching impact that extends beyond the midlatitude surf zone all the way to the subtropics. This vortex influence is clearly non-local so that even simple wave 2 distortions that leave the vortex well confined within the midlatitudes are observed to excite subtropical waves. Treating subtropical PV as active tracers also showed that upon entrainment, these large scale tongues of low PV air also influenced the dynamics of their own poleward migration.

### **Publications Based on UARS Research:**

- Hartley, D., J. Villarin, R. Black and C. Davis, A new perspective on the dynamical link between the stratosphere and troposphere, *Nature*, **391**, 471-474, 1998.
- Villarin, J., D. Hartley, and R. Black, Diagnosing the polar excitation of subtropical waves in the stratosphere, *J. Atmos. Sci.*, in review, 1999.
- Villarin, J., The Dynamical Influence of the Stratospheric Polar Vortex on the Atmospheric Global Circulation. Georgia Tech. PhD Thesis. 1997.
- Hartley, D. and R. Black, Preferred longitudinal regions of tropical/midlatitude mixing in the troposphere and lower stratosphere, EOS, Transactions, AGU, 76, pg F128, 1995.
- Villarin, J. and D. Hartley, The influence of polar vortex displacements on tropical-midlatitude exchange in the troposphere, EOS, Transactions, AGU, 76, pg F140, 1995.
- Hartley, D. and R. Black, Tropical/Midlatitude mass exchange in the troposphere, AMS/GOALS, Atlanta, 1996.

# Diagnosing the Polar Excitation of Subtropical Waves in the Stratosphere

Jose T. Villarín and Dana E. Hartley  
School of Earth and Atmospheric Sciences  
Georgia Institute of Technology  
Atlanta, Georgia

October 1997  
(Submitted to the Journal of Atmospheric Sciences)

Corresponding author address:  
Jose T. Villarín  
Manila Observatory  
Ateneo de Manila University  
Loyola Heights, Q.C.  
Philippines  
Email: jett@voir.eas.gatech.edu

## Abstract

The poleward migration of planetary scale tongues of subtropical air has often been associated with intense polar vortex disturbances in the stratosphere. This question of vortex influence is reexamined from a potential vorticity (PV) perspective. Anomalous geopotential height and wind fields associated solely with vortex PV anomalies are derived and their impact on the stratospheric subtropical circulation is evaluated. Combined PV inversion and Contour Advection (CA) calculations indicate that transient large scale disturbances of the polar vortex do have a far reaching impact that extends beyond the midlatitude surf zone all the way to the subtropics. This vortex influence is clearly non-local so that even simple wave 2 distortions that leave the vortex well confined within the midlatitudes are observed to excite subtropical waves. Treating subtropical PV as active tracers also showed that upon entrainment, these large scale tongues of low PV air also influenced the dynamics of their own poleward migration.

## 1. Context

In various observational and numerical analyses, the poleward entrainment of subtropical tongues of air has often been associated with intense vortex disturbances in the stratosphere (Leovy *et al.* 1985; Randel *et al.* 1993; Waugh 1993; Norton 1994; Polvani *et al.* 1995). Attributing the cause of this poleward subtropical transport to the polar vortex itself was a result of viewing time sequences of the vortex distortion and the subsequent subtropical wave breaking (e.g. Randel *et al.* 1993). Hence, one plausible mechanism hypothesized then was that during these vortex disturbances, the vortex edge is moved closer to the subtropics thereby entraining air parcels over there toward the midlatitudes.

However, in one recent study, Waugh (1996) concluded that equatorward incursions of the polar vortex may not at all be necessary for the poleward transport of subtropical air since transport out of the tropics was found to occur with or without the vortex. He thus proposed that the continuous breaking of subtropical waves is a result of upward and meridionally propagating Rossby waves incident on a nonlinear critical layer such as the surf zone (McIntyre and Palmer 1983, 1984). The crucial condition therefore for subtropical wave

breaking is not a perturbed polar vortex but a westerly regime that allows for the propagation of Rossby waves. The causal connection that was seen previously between vortex movement and subtropical wave breaking could thus be reinterpreted under a different light, i.e. that both events are probably two responses to one and the same “forcing” acting on the poleward and subtropical edges of the surf zone, rather than the former simply inducing the latter. This conclusion is further reinforced by contour advection (CA) calculations during periods which show continuous wave breaking in the polar regions despite the absence of the vortex.

In this study, we reexamine this question of vortex influence from a potential vorticity (PV) perspective. We ask whether or not waves confined to the high latitudes of the vortex edge can have a remote influence on the subtropics. The question itself is not entirely hypothetical since upward propagating planetary waves are observed to be refracted toward the polar latitudes during intense wave events in the polar vortex (e.g. Palmer 1981; Butchart *et al.* 1982; Kodera and Chiba 1995). Such planetary scale disturbances acting on the high PV gradients at the vortex edge create large scale PV anomalies that have associated circulations that may extend beyond the surf zone into the subtropics. If this is indeed the case, then the hypothesis of Waugh (1996) about the source of polar and subtropical wave breaking may have to be recast more subtly, taking into account the added feedback which polar wave events may have on subtropical wave growth.

We isolate the remote effect of polar perturbations on the subtropics by using the principle of PV invertibility (Hoskins *et al.* 1985). This allows us to derive or invert for the anomalous flows that can be attributed to various PV anomaly distributions in the atmosphere. We use quasi-geostrophic (QG) PV since its linearity allows a unique separation of geopotential height contributions coming from these PV anomalies (Robinson 1988; Hartley *et al.* 1997). This instantaneous association of geopotential height (hereafter referred to as height) with PV to infer the horizontal impact of vortex PV perturbations is complemented further by using CA calculations to analyze the evolution of subtropical material contours in time.

In the next section, the method of QGPV inversion is briefly described together with the observational data to which it is applied. The basic application of CA to analyze the temporal evolution of subtropical PV is also discussed here. Several vortex wave events for

the northern winter of 1992-93 are examined in subsequent sections. The wave event of 1 January 1993 is the focus of Section 3. More extensive analysis is purposely applied on this event so that it can serve as an analytical template upon which the discussion of other events will be based. Section 4 continues the analysis for the other wave events of this winter. The study concludes with a discussion of dynamical implications in the final section.

## 2. Method of Analysis

### a. Piecewise PV Inversion

In spherical geometry, the QG expression for PV is expressed as:

$$q = f + \widetilde{\nabla}^2 \Psi \quad (1)$$

where  $f$  is the Coriolis parameter,  $\Psi$  is the geostrophic streamfunction acted upon by the Laplacian-like operator  $\widetilde{\nabla}^2$ :

$$\widetilde{\nabla}^2 = \frac{1}{a^2 \cos^2 \phi} \frac{\partial^2}{\partial \lambda^2} + \frac{\tan \phi}{a^2} \frac{\partial}{\partial \phi} \left( \cot \phi \frac{\partial}{\partial \phi} \right) + \frac{f^2}{\pi^{2.5}} \frac{\partial}{\partial \pi} \left( \frac{\pi^{2.5}}{S} \frac{\partial}{\partial \pi} \right) \quad (2)$$

The independent vertical coordinate is the Exner function,  $\pi = C_p (p/p_0)^{R/C_p}$  and  $S$  represents the static stability of the QG reference state,  $S = -d\Theta(\pi)/d\pi$ . The dimension of  $q$  is  $\text{sec}^{-1}$  and its values can range from 0 to 3 QPVU (where  $1 \text{ QPVU} = 10^{-4} \text{ sec}^{-1}$ ) in the northern winter hemisphere.

The linearity of the operator in Eq. 2 suggests that  $\Psi$  or equivalently the geopotential  $\Phi$  (where  $\Phi = f\Psi$ ) can be uniquely associated with a given distribution of  $q$ , that is,

$$\Phi = f \widetilde{\nabla}^{-2}(q - f) \quad (3)$$

Through this invertibility between  $q$  and  $\Phi$ , various features that make up the total  $\Phi$  field can be attributed to particular components of the total  $q$  distribution. Thus, one can subdivide the total  $q$  field into any number of constituent  $q$  partitions and from these calculate the individual geopotential fields induced by these  $q$  partitions. The QG system has been shown

to be valid up to about 10 mb ( $\simeq 30$  km) (Boville 1987; Randel 1987) and has been verified in our calculations to be reasonable for the levels we have chosen ( $\simeq 30$  mb).

In practice, it is the height ( $Z$ ) contribution due to specific  $q$  distributions in the atmosphere that is calculated in the inversion process. First,  $q$  and  $Z$  are decomposed into their time mean and perturbation components. Such decomposition allows the separation of the flow field into its transient and stationary features. An anomaly here is defined to be a transient departure from the wintertime mean state. Thus, if  $q = \bar{q} + \widetilde{\nabla}^2(gZ/f)$  and  $\bar{q} = \bar{f} + \widetilde{\nabla}^2(g\bar{Z}/f)$ , then

$$q' = \widetilde{\nabla}^2(gZ'/f) \quad \text{or} \quad Z' = (f/g) \widetilde{\nabla}^{-2}q' \quad (4)$$

where the bar and prime symbols denote the seasonal time mean and deviation from this mean, respectively. Transient height anomalies at some level, such as 32 mb, can therefore be attributed to the transient distribution of  $q$ .

This transient  $q$  anomaly field can be horizontally partitioned into components that belong to the polar vortex and to regions outside the vortex. Thus,

$$Z' = (f/g) \widetilde{\nabla}^{-2}(q'_{\text{vortex}} + q'_{\text{extra-vortex}}) \quad (5)$$

The inversion of  $q$  anomalies associated solely with the vortex allows us to distinguish the contribution of the transient vortex disturbance to the total height anomaly field from that attributed to extra-vortex PV anomalies.

PV anomalies associated with vortex changes are identified by using a simple masking scheme to separate vortex PV contours from the rest. In contrast to Ertel PV, the QG form of PV makes it possible to apply this separation at various vertical levels. To illustrate this point, Fig. 1 shows the 32 mb QG PV profile of a vortex wave event on 1 January 1993. PV contours poleward of the 1.1 QPVU line are identified with the vortex while those equatorward of 0.7 QPVU with the subtropics. That such a labeling scheme is valid for other levels in the stratosphere can be seen from the deep vertical extension of these contours in Fig. 2. In this Figure, latitude-height cross sections of PV for this wave event are plotted at the longitudes where the large scale transient trough and ridge are observed (110°E and

46°E, respectively). The designation of 1.1 QPVU as the vortex edge line (denoted by the bold contour at high latitudes) is conservatively chosen to be within the region of large PV gradients that mark the boundary of the polar vortex. This designated line is observed to bound the vortex over a deep layer from 100 to 10 mb. To mask out extra-vortex contours, the gridpoints containing QPVU values less than the vortex edge line for the wave event and the time mean are uniquely flagged and later set to zero when the PV anomalies are inverted.

### *b. Inversion Domain and Data*

The PV inversion was applied on the United Kingdom Meteorological Office (UKMO) analyzed data set for the boreal winter of 1992-93 (Swinbank and O'Neill 1994). This data set has a longitudinal and latitudinal resolution of 3.75° and 2.5° respectively. Nineteen vertical levels (1000 to 1.0 mb) that are equidistant in log pressure comprise the PV inversion domain.

The inversion was applied over a hemisphere which meant that horizontal boundary conditions had to be zonally cyclic and continuous over the pole. Polar continuity was possible using the method of Haltiner and Williams (1980). The only lateral boundary condition was at the low latitude limit where QG theory breaks down. At this low latitude limit (15°N), the Dirichlet boundary condition,  $\Phi' = 0$ , was applied.

The non-zero  $\theta'$ , where  $\theta' = -\partial\Phi'/\partial\pi$ , was used as the vertical boundary condition whenever the surface or top level PV was included in the inversion. Otherwise, the Neumann boundary condition,  $\partial\Phi'/\partial\pi = 0$ , was applied when interior PV was inverted (Davis 1992; Davis and Emanuel 1991).

### *c. Contour Advection*

As Eq. 5 suggests, different sets of height anomaly fields can be derived from several PV anomaly partitions. In this study, two sets of height anomaly fields are compared, namely the “total” height anomaly field, i.e. that associated with both vortex and extra-vortex PV anomalies, and the “vortex” height anomaly field, i.e. that associated solely with polar vortex disturbances. Both sets of height fields are instantaneous snap shots of the atmospheric flow

produced accordingly by these different PV partitions on the wave event of interest.

Such a comparison of both height fields already gives us an idea of the instantaneous impact of vortex perturbations on the atmospheric flow. This impact can be examined further by tracing the temporal evolution of material contours as these are advected by winds associated with both sets of height fields. For this, the CA method is used to study how subtropical contours evolve under different wind regimes associated with these height fields.

CA calculations have been employed successfully in previous studies that have examined the fine scale evolution of material contours in the stratosphere (Waugh and Plumb 1994; Plumb *et al.* 1994; Waugh *et al.* 1994). In this study, the CA routine is initialized several days before the mature wave event, on a day usually marked by transient wave quiescence. PV inversions are then performed from this initial day up to the wave event itself to obtain the daily wind fields needed for the CA routine.

The first CA calculation is done by advecting a specific subtropical PV contour with the vortex wind field that is obtained from the stationary (time mean) wind plus the transient wind due solely to vortex PV anomalies. The resulting contour evolution can then be examined for any evidence of entrainment or filamentation that may be directly associated with transient vortex PV disturbances. A second CA calculation advects the same subtropical contour with the total wind field obtained from the background stationary flow and the full set of unpartitioned (i.e. vortex plus extra-vortex) PV anomalies. Comparing the two final pictures that emerge from these calculations enables us to see the dynamical contribution of vortex and extra-vortex (or largely subtropical) PV anomalies on the subsequent transport of subtropical air. A contour length diagnostic is used to quantify the comparison.

### 3. The Wave Event of 1 January

#### *a. Dynamically Significant PV Levels*

According to the PV profile of Fig. 1, the vortex wave event on this day is characterized by a typical wave 2 perturbation with PV troughs over the North Atlantic and northern China, and ridges over eastern Europe and the Aleutians. Associated with this vortex

distortion are tongues of subtropical air moving poleward at those regions south and east of the vortex PV troughs.

Subtracting the time mean or stationary component from the total fields for this day produces the PV and height anomaly fields in Fig. 3. The various contributions to the total height anomaly field at this particular level can be attributed to different components of the PV anomaly distribution at several regions and levels in the atmosphere. Thus, in order to capture the flow and its salient features, it is necessary to determine the location of those PV anomalies that are important in terms of their contribution to the flow at the level of interest which, in this case, is the 32 mb level. This is done by individually inverting the PV anomalies at all levels in the atmosphere to obtain the height anomaly field associated with each level. The superposition of all these height anomaly contributions coming from different levels should yield the total height anomaly field at 32 mb.

To quantify the contribution of PV anomalies at various levels to the height anomaly field at 32 mb, a quantity somewhat akin to the normalized covariance of both the induced height contribution and the total height field (Robinson 1988) is calculated. Such a contribution or weighting coefficient ( $C$ ) is mathematically expressed as:

$$C(z_0, z) = \frac{\iint \phi^z(x, y, z_0) \Phi(x, y, z_0) dA}{\iint \Phi(x, y, z_0)^2 dA} \quad (6)$$

where  $\Phi$  is the total height anomaly at the level of interest ( $z_0$ ) that is due to all the PV in the atmosphere, and  $\phi^z$  is the height anomaly at level  $z_0$  that is due to the PV distribution at the variable level  $z$ . The area integrals in the fraction denote that the heights are areally weighted over a hemisphere.

In addition to calculating the individual contribution coefficient, one can likewise calculate the cumulative contribution of PV to the total height anomaly at  $z_0$ . This only requires modifying  $\phi$  in Eq. 6 to denote the height anomaly contribution to  $z_0$  that is due to PV anomalies at successive levels from the surface ( $z = 0$ ) up to the specified level  $z$ .

Both individual and cumulative contribution coefficients are shown in Fig. 4 which illustrates the dynamical significance of PV at altitudes that are close to the level of interest (32 mb). This confirms what Robinson (1988) concluded about the greater importance of

local PV over remote PV distributions in determining the total flow at a particular level in the stratosphere. Thus, from Fig. 4a, the strongest contribution to the 32 mb height field comes from the PV anomalies at this level itself. When the cumulative contribution coefficient is plotted in Fig. 4b, it is evident that the height field induced by PV anomalies from the surface up to 32 mb only accounts for 60% of the total height anomaly field at 32 mb. This total field is only completely accounted for with the inclusion of PV at stratospheric levels above 32 mb.

Furthermore, the cumulative contribution of tropospheric PV anomalies on the 32 mb level effectively cancels out and only those PV structures starting at around 15 km begin to contribute significantly to the 32 mb flow. Of course, this is not to imply that tropospheric PV has no effect on the middle stratosphere whatsoever. In the first place, the large scale stratospheric PV anomalies are generated largely by upward propagating planetary disturbances that originate from the troposphere. What the contribution coefficients illustrate simply is a diagnostic weighting procedure to measure the relative contributions of these PV anomalies to the instantaneous flow at the 32 mb level. Thus, from these contribution coefficients, we conclude that at a particular point in time such as the wave event of this day, the PV anomalies at levels spanning the 100 to 10 mb levels are dynamically important in determining the total anomalous flow at 32 mb.

### *b. Vortex PV Inversion*

The results of the PV inversion for this event are shown in Fig. 5. Three PV anomaly configurations on the 32 mb level are plotted on the left column and inverted height anomalies on the right. For example, Fig. 5b shows the result of inverting not just the PV anomaly distribution shown in Fig. 5a but all the PV anomalies within the 100 to 10 mb levels. For convenience, not all the PV levels are shown and the 32 mb distribution is selected to be representative of the rest. As shown previously, it is the PV field at this level that dominates the 32 mb height field. The similarity between the inverted height anomaly field of Fig. 5b and that of the total height anomaly field of Fig. 3b demonstrates how the 32 mb flow is captured effectively by PV anomalies spanning the 100 to 10 mb range.

The second and third rows of Fig. 5 show the results of horizontally partitioning the

total PV structure represented by Fig. 5a into its vortex and extra-vortex components. Thus in Fig. 5c, only PV anomalies associated with the vortex disturbance are shown. Adjacent to this, in Fig. 5d, are the height anomalies that result from inverting only these vortex PV at the dynamically significant levels (100-10 mb). The similarity between Fig. 5d and Fig. 5b illustrates the dominant influence of the polar vortex in the dynamics of the winter stratosphere at this level. The significance of any residual or extra-vortex influence on this level is shown in Fig. 5e and Fig. 5f which illustrate the effect of PV structures beyond the vortex region.

The influence of extra-vortex PV is largely attributed to subtropical PV that has been advected poleward into the midlatitude surf zone. Since the midlatitude surf zone is marked by low PV gradients, PV disturbances found in this region outside the polar vortex are associated mostly with vortex and subtropical material entrained into the midlatitudes. The PV anomalies associated with the subtropics arise largely from perturbations of the subtropical edge of the surf zone. This edge is marked by PV gradients that are not as steep as those at the vortex edge but are nevertheless important. Thus, incursions of subtropical air into the midlatitudes create negative PV anomalies in the midlatitude surf region which, upon inversion, produce the broad expanse of positive height contributions that extend from the subtropics to the high latitudes shown in Fig. 5f.

The effect of this broad expanse of positive height anomalies, induced by subtropical PV, on the instantaneous total height anomaly field can be seen by comparing Fig. 5b and Fig. 5d. There are subtle differences that can be attributed to extra-vortex PV. For instance, the large scale cyclonic circulation over the North Atlantic that is induced by the anomalous equatorward movement of one portion of the vortex extends farther to the south and has a larger amplitude when the influence of the subtropics is not considered (Fig. 5d). On the other hand, the anticyclonic circulation over northern Europe extends further south and its amplitude increases when extra-vortex PV anomalies are included in the calculation of the total height anomaly field. This suggests that while vortex PV perturbations dominate the dynamics of the winter stratosphere, subtropical PV anomalies entrained into the midlatitudes modify this vortex influence.

The height anomaly fields shown in Fig. 5 already give us an idea of the extent of the

horizontal influence of vortex disturbances throughout the stratosphere. To examine whether these height anomalies have any impact at all on the excitation and eventual entrainment of subtropical waves, wind fields derived from these heights will now be used to advect subtropical contours in time.

### *c. Subtropical Entrainment*

The entrainment of subtropical material contours due to vortex perturbations is possible only if the winds associated with the vortex PV anomalies are large and extensive enough to sustain the poleward movement of these contours. CA calculations provide us a method of examining the effectiveness of such a wind field in bringing about subtropical transport. The material contour that is advected is the PV contour that corresponds to the subtropical edge of the surf zone (0.7 QPVU). Two sets of wind fields are used to advect this contour: the total wind field (i.e. stationary plus transient winds due to all the significant PV anomalies in the stratosphere) and the anomalous or vortex wind field (stationary plus transient winds due only to vortex PV perturbations). For convenience, the entrainment of subtropical contours due to each set of wind fields is labeled total and vortex entrainment, respectively.

For the event of 1 January, the evolution of the subtropical PV contour under the action of the vortex wind field is shown in Fig. 6. The CA calculation is initialized five days before the mature phase event. What is immediately obvious from these plots are the tongues of subtropical air entrained along the cyclonic circulation patterns associated with the vortex distortion. Substantial extrusions of subtropical air into the midlatitudes are found over Japan and the eastern Atlantic. The remote effect of these high latitude perturbations on the subtropics is clearly evident despite the confinement of vortex PV anomalies to the middle and high latitudes.

To see how differently the contours would evolve if extra-vortex PV were included, another set of CA calculations were made, this time, using the total wind field associated with the full unpartitioned PV structures. The evolution of these subtropical contours is traced in Fig. 7. Since this calculation advects the contours with the total winds, the final result should simulate at least the observed coarse grain picture of Fig. 1. Large scale

features of the high resolution calculation do in fact correspond to the observed subtropical PV contours. Differences are to be expected due to numerical integration errors and the fact that only the PV structures spanning the 100 to 10 mb levels were inverted in deriving the wind fields. The contour evolution of Fig. 7 shows the same qualitative features of poleward entrainment as in Fig. 6 with some subtle differences that can be attributed to extra-vortex PV.

The effect of extra-vortex PV on subtropical wave breaking, which essentially is a self-advective effect, can be gleaned from the differences between the pictures of Fig. 6 and Fig. 7. Vortex entrainment over Japan (Fig. 6) shows a northeastward meridional slant of the subtropical contour as a result of the cyclonic circulation produced by the positive vortex PV anomaly in this region. When the influence of subtropical PV is included in the advection, total entrainment over this region (Fig. 7) is more zonally extended with enhanced troughing observed downstream of the tongues. Vortex entrainment over the Atlantic shows the same characteristic meridional slant. Total entrainment appears to lead to greater thinning or filamentation of contours. The filamentation itself is accompanied by enhanced troughing downstream of these entrained tongues. Moreover, under total entrainment, these wave crests are located slightly more westward, suggesting that the effect of subtropical PV on itself is to propagate upstream. Under vortex entrainment, these subtropical PV anomalies would simply be advected poleward and downstream like any passive tracer.

This largely qualitative and visual analysis can be complemented further by measuring the length of these evolving contours to diagnose the degree of wave breaking and irreversible transport. Irreversible deformation of these contours is evaluated by comparing contour lengths corresponding to both total and vortex entrainment with the initial (pre-event) contour state. The time rate of change of these contour lengths can be used as a diagnostic for transport. Chen (1996) used the lengthening rate of these material contours as an indicator of wave breaking. The lengthening rate equation is reproduced here:

$$\gamma = \frac{1}{(t_{final} - t_{initial})} \ln \left[ \frac{L(t_{final})}{L(t_{initial})} \right]$$

where  $t_{final}$  and  $t_{initial}$  denote the time interval between the initial and final states of contour

advection, and  $L$  represents the length of the material contours at each of these states. It is the exponential rate of lengthening that is used as a diagnostic of rapid mixing and wave breaking rather than the linear increase in contour lengths (Chen 1996 and references therein). We adopt the same  $\gamma$  value of  $0.05 \text{ day}^{-1}$  as a threshold for this wave breaking. Such a threshold implies a 12-fold increase in the length of a material line in 50 days or a doubling of length in 14 days. Wave breaking itself does not necessarily imply the literal fracturing of material lines; rather, it refers to the irreversible deformation of PV material contours in contrast to the simple linear undulation of a Rossby wave (Holton *et al.* 1995). For these advected contours, an increase in filamentation and their subsequent evolution into smaller scales lead to greater probability of irreversible mixing.

A summary of contour length diagnostics for this and other wave events of this study is shown in Table 1. Under vortex entrainment, the subtropical contour for the wave event of 1 January increases by 37% in a matter of five days. This corresponds to a lengthening rate of .06 per day which is above our threshold for irreversible deformation and wave breaking. The spatial extent and strength of the vortex wind field is therefore enough to bring about the extrusion of subtropical material into the extratropics. Under total entrainment, both the fractional length increase and the lengthening rate are even larger (63% and .10 respectively), suggesting the enhancement of subtropical wave breaking by the subtropical PV anomalies themselves.

## 4. Other Wave Events

### a. 9 January

The wave event of this day is a wave 2 perturbation with a vortex orientation similar to the previous wave event just analyzed. The location of vortex ridges and troughs together with their associated circulations are approximately collocated with those of the previous event. CA calculations are initialized six days before the mature wave event and the result shown in Fig. 8.

The influence of vortex PV on the subtropics can be seen in the prominent spike of subtropical material over the western Pacific. Other subtropical waves are observed to be

excited downstream of this spike in the central Pacific and over the eastern Atlantic and North Africa. When the effect of extra-vortex PV is considered (under total entrainment), the subtropical contour over East Asia and the western Pacific is even more distorted with a thin filament extending poleward all the way to the Aleutians. Increased zonality is also seen in the way subtropical filaments are entrained particularly over Japan. In this region, filaments of midlatitude PV air are also seen to intrude zonally into the subtropical reservoir over Taiwan. The trough over North Africa, in the case of total entrainment, is simply absent under vortex entrainment, suggesting again that the effect of a subtropical PV anomaly on its own development is to propagate upstream, or more precisely, to induce an anticyclonic circulation that tends to create a trough on its east flank and a ridge on its west flank. This tendency for a subtropical PV anomaly to propagate upstream may readily dominate over its downstream advection because the background westerly flow over this subtropical region is weaker than at higher latitudes.

Another interesting feature of this event is that not only can the vortex induce poleward transport of subtropical material, it can also advect high latitude subtropical contours equatorward. This is clearly seen in Fig. 8b where the subtropical PV blob initially over the North Pacific and Alaska is brought closer to the U.S. subtropics due to the cyclonic circulation induced by the vortex trough over the northeast U.S. and Canada.

Contour length diagnostics (Table 1) show that vortex entrainment is enough to bring about the poleward transport of subtropical material, with a 70% increase in contour length over 6 days, corresponding to a lengthening rate of .09 per day. Under total entrainment, the contour length nearly doubles in that same span of time with much of the length increase occurring most probably over the highly distorted region in the western Pacific and East Asia. The lengthening rate under total entrainment (.11 per day) is more than twice that of our threshold.

### *b. 16 February*

The vortex event of this day is a wave 1 perturbation with an anomalously intense Aleutian ridge and a polar vortex displaced over Europe. The results of CA calculations, initialized six days prior to this wave event, are shown in Fig. 9. A broad extrusion of

subtropical air due solely to vortex PV is seen over the North Pacific extending all the way from Far East Asia across the Arctic into the northwest U.S. This large scale subtropical extrusion goes along the interface between the Aleutian High and the polar vortex low. When the vortex is displaced equatorward, anomalously low and high PV distributions simultaneously arise, creating a PV anomaly dipole structure in the polar atmosphere. At the juncture of this dipole are enhanced winds running transverse to the dipole's axis which are associated with the intense PV gradients created by the presence of both PV anomaly poles. By PV inversion, the lateral extent of these enhanced winds is found to be large enough to encompass both the midlatitude surf zone and its subtropical edge. It is this enhanced anomalous wind structure, associated with vortex PV anomalies, that is mainly responsible for the extensive poleward entrainment of subtropical air.

Under total entrainment, this subtropical extrusion induced by polar PV is modified in several ways. As with other events, the dynamical effect of subtropical PV on its own poleward movement shows a marked increase in filamentation, as suggested by the much thinner tongue and the way the tip of this tongue is chaotically entwined around the Aleutian region. The subtropical region from which this extrusion originates is again found to be more westward of where it would be if only vortex PV anomalies determined the subtropical flow. Extensive troughing is also observed all over the Pacific and immediately eastward of the subtropical tongue. Some form of retardation can be observed from the manner in which the minor contour initially situated near Russia wraps around the vortex edge.

Contour length calculations (Table 1) confirm again the strength of vortex influence on subtropical entrainment, showing a contour length fractional increase of 57% and a lengthening rate of .08 per day within a span of six days. Under total entrainment, the length of this initial contour increases to 74% within this same time interval. The small increase in lengthening rate (from .08 to .09) suggests the sheer dominance of vortex PV perturbations alone in bringing about subtropical wave breaking.

### *c. 6 March*

The wave 1 perturbation event of this day shows the same qualitative features of the previous wave event. In the 18 days that transpired from that wave event to this day, the

highly disturbed vortex was observed to rotate about  $225^\circ$  downstream. On this day, the rotated vortex is displaced over Russia with an intense positive height anomaly centered over Canada. Such a configuration leads to a dipole structure of large scale positive and negative PV anomalies. Fig. 10 shows the results of the CA calculation, initialized six days prior to the mature wave event. Readily observable from the plots of Fig. 10b and Fig. 10c are the subtropical intrusions along the corridor marking the interface between the low and high PV centers over Canada and Russia respectively.

The dynamical influence of vortex PV alone on subtropical transport is seen not only from these long filaments over the subtropical western Pacific that extend from the subtropics all the way to the Arctic, but also from wave crests found over Africa and Mexico. Interestingly enough, the direction of wave cresting over Mexico is different from that over Africa. The southeast to northwest tilt of these wave crests over Mexico is due to the large scale anticyclonic circulation centered over Canada. The southwest to northeast tilt of the African subtropical spike is associated with the cyclonic circulation of the displaced vortex.

Under total entrainment, the distinct contribution of subtropical PV to its own poleward movement can be observed. In Fig. 10c, the subtropical contour over the western Pacific shows several tongues pointing toward the north. The spatial extent of these tongues seems to be influenced also by the neighboring large scale anticyclonic circulation associated with the subtropical PV blob centered over Canada. Enhanced troughing is again observed immediately downstream of these tongues. Another subtropical tongue can be observed over the eastern Atlantic with some troughing east of the extrusion. Under total entrainment, the region of subtropical extrusion is also located upstream of where it would be under simple vortex entrainment. The tilt of the wave crests over Mexico is not as apparent under total entrainment. Another interesting feature is the difference in the way the minor subtropical contour, initially centered over the Aleutians, wraps itself anticyclonically around the center of high pressure (Canadian High). Under total entrainment, this wrap around process is much more enhanced because of a high pressure center reinforced by low PV contributions entrained from the subtropics. This high pressure center has been observed to remain relatively isolated for more than a week, leading to a pocket of low ozone that has been discovered in this region (Manney *et al.* 1995).

The results of contour length calculations (Table 1) show values that are similar to those of the previous wave event. Under vortex entrainment alone, the subtropical contour is lengthened by 58% in a span of six days, thus leading to a lengthening rate of .08 per day, still above the threshold for wave breaking. Under total entrainment, these values are increased slightly further to 73% and .09, again showing the dominance of vortex PV perturbations in bringing about the poleward transport of subtropical air.

## 5. Discussion/Conclusion

The overall conclusion that can be drawn from all this analysis is that transient large scale perturbations of the stratospheric polar vortex do have a far reaching impact that extends all the way to the subtropics. Furthermore, piecewise PV inversion has demonstrated that this remote influence need not require the vortex edge to touch low latitudes as may be expected in some wave 1 vortex displacement events. Even simple wave 2 distortions that leave the vortex well confined within the middle latitudes are observed to have an appreciable effect on the dynamics of subtropical transport. CA calculations coupled with contour length diagnostics suggest the sheer dominance of this vortex influence not only on the high or midlatitude stratosphere but on the poleward entrainment of subtropical air as well.

This of course does not imply that the vortex is the sole cause of subtropical wave excitation and/or breaking. As Waugh (1996) clearly pointed out, instances of transport out of the subtropics are found to occur rather independently of a polar vortex for as long as westerly flow allowed the upward propagation of Rossby waves. Subtropical waves arise then out of vertically propagating Rossby waves that eventually break on the subtropical edge of the surf zone. What we have shown here is that during vortex wave events at least, perturbations on the poleward edge of the surf zone can excite ripples and filaments along the equatorward edge of this surf zone. Quantitative analysis further suggests that a significant fraction of these subtropical tongues is associated with the horizontal influence of vortex PV disturbances. With or without Rossby waves moving upward and breaking on the subtropical edge of the surf zone, this feedback effect coming from disturbances on the

vortex edge cannot be neglected.

Once this remote influence of the vortex waves is taken into account, the total transport of subtropical air is not a simple matter of passive advection by the winds associated with vortex entrainment. Since PV itself is a dynamic tracer, its advection and resulting redistribution will influence subsequent development of the atmospheric flow. This distinct advantage of using PV as an active tracer allows us to draw a dynamical picture of the transport process associated with the coupled interaction of vortex and subtropical PV anomalies. This picture is schematically shown in Fig. 11. Assuming that the wave disturbance is focused solely on the high PV vortex edge (Fig. 11a), a subtropical, low PV pulse can arise as a consequence of the laterally extensive circulations associated with the vortex PV anomaly (Fig. 11b). Both pulses lead to a positive PV anomaly in the high latitudes and a negative PV anomaly in the subtropics. The cyclonic circulation induced by the positive PV anomaly at the vortex edge can, by itself, advect subtropical material into the midlatitudes, i.e. vortex entrainment alone is efficient enough to excite subtropical waves and entrain subtropical material into the wave breaking region of the surf zone.

The total dynamical picture however includes these negative subtropical PV anomalies that are entrained into the midlatitudes. Because the PV gradients in the subtropical edge of the surf zone are not as strong as those at the polar edge, these negative PV anomalies are generally smaller in amplitude and spatial scale. Despite this however, differences we have seen between vortex entrainment and total entrainment suggest that the circulations associated with these subtropical PV anomalies are not negligible. One non-negligible effect of entrained subtropical PV is to tighten the height gradient along the interface that separates it from the positive vortex PV anomaly. As Fig. 11c suggests, such gradient tightening leads to the possibility of increased wind magnitudes along this corridor. This self-advective effect, owing to the dynamic nature of PV, also results in the enhanced troughing immediately east of these subtropical PV anomalies. The coupling of the vortex induced cyclonic circulation with the subtropical anticyclonic circulation may also lead to greater diffuent flow past the region of tight gradients. Hence instead of assuming a northeastward trajectory as a result of the cyclonic sweep of the vortex PV anomaly, the subtropical filament takes on a more eastward or zonal orientation because of the added influence of the subtropical PV.

The subtropical PV anomalies being considered here are only those associated with the subtropical edge of the surf zone that wind up in the extratropics as a result of vortex entrainment. There are certainly extraneous subtropical and tropical PV anomalies not associated with vortex entrainment but because of their weak amplitudes and scale, their dynamical influence will most likely be confined within the subtropical reservoir.

Among the regions that show poleward subtropical entrainment, CA calculations indicate a preferred location for substantial subtropical extrusions, namely over Japan and the Western Pacific. Interestingly enough, in this preferred region (for example, on the 1 January event), transient or anomalous heights over this region are weaker in amplitude and less extensive than the other cyclonic center over the North Atlantic (see Fig. 5d).

This preferred region of subtropical wave breaking could be due to zonal differences in the steepness of the subtropical PV gradient. Another possible reason for this region of persistent entrainment is the action of stationary waves. The stationary eddy configuration at the 32 mb level is marked by two planetary scale cyclonic circulation patterns over Russia and Greenland. The stationary troughs over the former are more extensive and have larger amplitudes than the latter. In fact, preliminary CA calculations (not shown) which use stationary winds to advect zonally symmetric subtropical contours yielded some poleward extrusions over this preferred region in the Pacific. Future PV studies will need to separate the influences due to stationary and transient eddies on subtropical transport. A potentially important consequence of this preferred region of transport is the feeding of the Aleutian High with low PV subtropical air through horizontal transport.

### *Acknowledgements*

We thank C. Davis of NCAR, D. Waugh of CRC SHM (Australia), and M. Nakamura (MIT) for setting the groundwork for the PV and CA calculations. This work was sponsored by NASA Grant NAG5-2789.

## References

- Boville, B. A., 1987: The validity of the geostrophic approximation in the winter stratosphere and troposphere. *J. Atmos. Sci.*, **44**, 443–457.
- Butchart, N., S. A. Clough, T. N. Palmer, and P. J. Trevelyan, 1982: Simulations of an observed stratospheric warming with quasigeostrophic refractive index as a model diagnostic. *Quart. J. Roy. Meteor. Soc.*, **108**, 475–502.
- Chen, P., 1996: The influences of zonal flow on wave breaking and tropical-extratropical interaction in the lower stratosphere. *J. Atmos. Sci.*, **53**, 2379–2392.
- Davis, C. A., 1992: Piecewise potential vorticity inversion. *J. Atmos. Sci.*, **49**, 1397–1411.
- Davis, C. A. and K. A. Emanuel, 1991: Potential vorticity diagnostics of cyclogenesis. *Mon. Wea. Rev.*, **119**, 1929–1953.
- Haltiner, G. J. and R. T. Williams, 1980: *Numerical Prediction and Dynamic Meteorology*. Wiley.
- Hartley, D. E., J. T. Villarín, R. X. Black, and C. A. Davis, 1997: A new perspective on the dynamical link between the stratosphere and troposphere. *Nature*, in review.
- Holton, J. R., P. H. Haynes, M. E. McIntyre, A. R. Douglass, R. B. Rood, and L. Pfister, 1995: Stratosphere-troposphere exchange. *Rev. Geophys.*, **33**, 403–439.
- Hoskins, B. J., M. E. McIntyre, and A. W. Robertson, 1985: On the use and significance of isentropic potential vorticity maps. *Quart. J. Roy. Meteor. Soc.*, **111**, 877–946.
- Kodera, K. and M. Chiba, 1995: Tropospheric circulation changes associated with stratospheric sudden warmings: A case study. *J. Geophys. Res.*, **100**, 11055–11068.
- Leovy, C. B., C.-R. Sun, M. H. Hitchman, E. E. Remsberg, J. M. Russell, L. L. Gordley, J. C. Gille, and L. V. Lyjak, 1985: Transport of ozone in the middle atmosphere: Evidence for planetary wave breaking. *J. Atmos. Sci.*, **42**, 230–244.

- Manney, G. L., L. Froidevaux, J. W. Waters, R. W. Zurek, J. C. Gille, J. B. Kumer, J. L. Mergenthaler, A. E. Roche, A. O'Neill, and R. Swinbank, 1995: Formation of low-ozone pockets in the middle stratospheric anticyclone during winter. *J. Geophys. Res.*, **100**, 13939–13950.
- McIntyre, M. E. and T. N. Palmer, 1983: Breaking planetary waves in the stratosphere. *Nature*, **305**, 593–600.
- McIntyre, M. E. and T. N. Palmer, 1984: The 'surf zone' in the stratosphere. *J. Atmos. Terr. Phys.*, **46**, 825–849.
- Norton, W. A., 1994: Breaking Rossby waves in a model stratosphere diagnosed by a vortex-following coordinate system and a technique for advecting material contours. *J. Atmos. Sci.*, **51**, 654–673.
- Palmer, T. N., 1981: Diagnostic study of a wavenumber-2 stratospheric sudden warming in a transformed Eulerian-mean formalism. *J. Atmos. Sci.*, **38**, 844–855.
- Plumb, R. A., D. W. Waugh, R. J. Atkinson, P. A. Newman, L. R. Lait, M. R. Schoeberl, E. V. Browell, A. J. Simmons, and M. Loewenstein, 1994: Intrusions into the lower stratospheric Arctic vortex during winter of 1991–1992. *J. Geophys. Res.*, **99**, 1089–1105.
- Polvani, L. M., D. W. Waugh, and R. A. Plumb, 1995: On the subtropical edge of the stratospheric surf zone. *J. Atmos. Sci.*, **52**, 1288–1309.
- Randel, W. J., 1987: The evaluation of winds from geopotential height data in the stratosphere. *J. Atmos. Sci.*, **44**, 3097–3120.
- Randel, W. J., J. C. Gille, A. E. Roche, J. B. Kumer, J. L. Mergenthaler, J. W. Waters, E. F. Fishbein, and W. A. Lahoz, 1993: Stratospheric transport from the tropics to middle latitudes by planetary-wave mixing. *Nature*, **365**, 533–535.
- Robinson, W. A., 1988: Analysis of LIMS data by potential vorticity inversion. *J. Atmos. Sci.*, **45**, 2319–2342.

- Swinbank, R. and A. O'Neill, 1994: A stratosphere-troposphere data assimilation system. *Mon. Wea. Rev.*, **122**, 686–702.
- Waugh, D. W., 1993: Subtropical stratospheric mixing linked to disturbances in the polar vortices. *Nature*, **365**, 535–537.
- Waugh, D. W., 1996: Seasonal variation of isentropic transport out of the tropical stratosphere. *J. Geophys. Res.*, **101**, 4007–4023.
- Waugh, D. W. and R. A. Plumb, 1994: Contour advection with surgery: A technique for investigating finescale structure in tracer transport. *J. Atmos. Sci.*, **51**, 530–540.
- Waugh, D. W., R. A. Plumb, R. J. Atkinson, M. R. Schoeberl, L. R. Lait, P. A. Newman, M. Loewenstein, D. W. Toohey, L. M. Avallone, C. R. Webster, and R. D. May, 1994: Transport out of the lower stratospheric Arctic vortex by Rossby wave breaking. *J. Geophys. Res.*, **99**, 1071–1088.

Table 1. Contour Diagnostics Corresponding to Initial, Vortex, and Total Entrainment.  
 Contour Diagnostics Corresponding to Initial, Vortex, and Total Entrainment.

	Length ( $10^7$ m)	% Increase	Length Rate ( $\text{day}^{-1}$ )
<i>1 Jan</i>			
Initial	5.42		
Vortex	7.42	37	.06
Total	8.85	63	.10
<i>9 Jan</i>			
Initial	6.51		
Vortex	11.08	70	.09
Total	12.96	99	.11
<i>16 Feb</i>			
Initial	7.03		
Vortex	11.04	57	.08
Total	12.22	74	.09
<i>6 Mar</i>			
Initial	6.72		
Vortex	10.62	58	.08
Total	11.59	73	.09

## List of Figures

- 1 PV profile on 1 January at the 32 mb level. Light and dark shades denote vortex and subtropical areas bounded by the 1.1 and 0.7 QPVU line respectively. Contour interval is 0.1 QPVU.
- 2 Latitude-height cross section at the (a) trough region ( $110^{\circ}\text{E}$ ) and (b) ridge region ( $46^{\circ}\text{E}$ ) on 1 January.
- 3 (a) PV anomaly and (b) height anomaly fields at 32 mb level for the wave event of 1 January. Light and dark shades denote positive and negative values, respectively.
- 4 (a) Individual contribution of different levels and (b) cumulative contribution to the 32 mb flow.
- 5 (a) Total PV anomaly structure and its partitioned elements, (c) vortex PV and (e) extravortex PV. Inverted height results are to the right of each representative PV partition (b,d,f).
- 6 Evolution of subtropical contours under vortex entrainment. Numbers indicate the day of integration, from 28 December to 1 January.
- 7 Same as in Fig. 6 but for total entrainment.
- 8 (a) Initial subtropical contour state, (b) final evolution under vortex entrainment, and (c) final evolution under total entrainment for the event of 9 January.
- 9 Same as in Fig. 8 but for the wave event of 16 February.
- 10 Same as in Fig. 8 but for the wave event of 6 March.
- 11 Schematic diagram of the transport mechanism generated by vortex perturbations.



Fig. 1

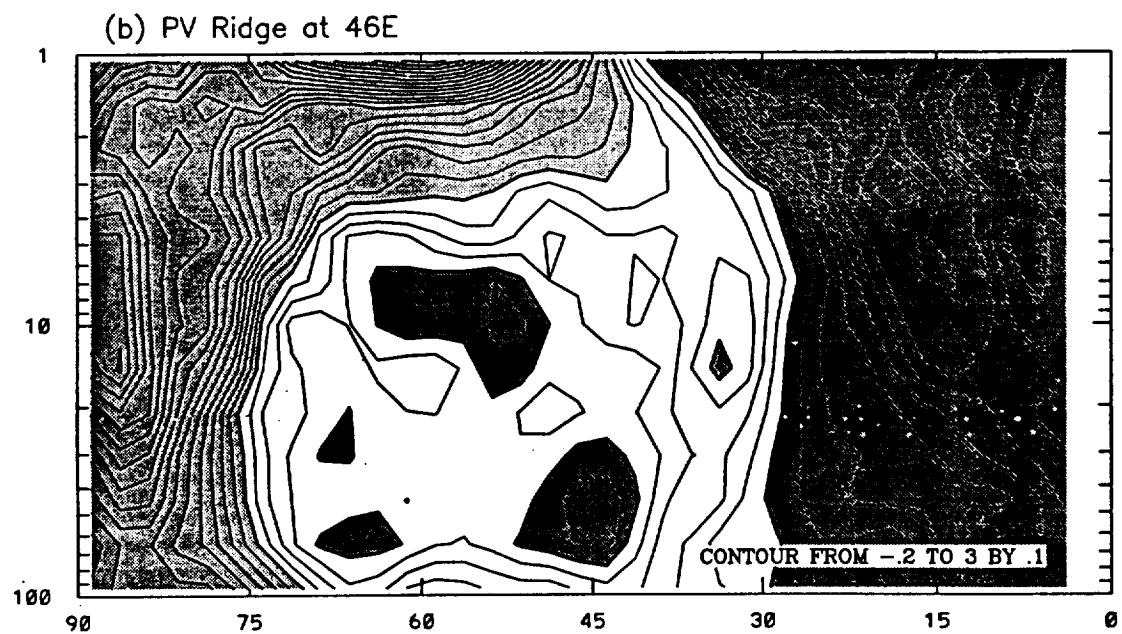
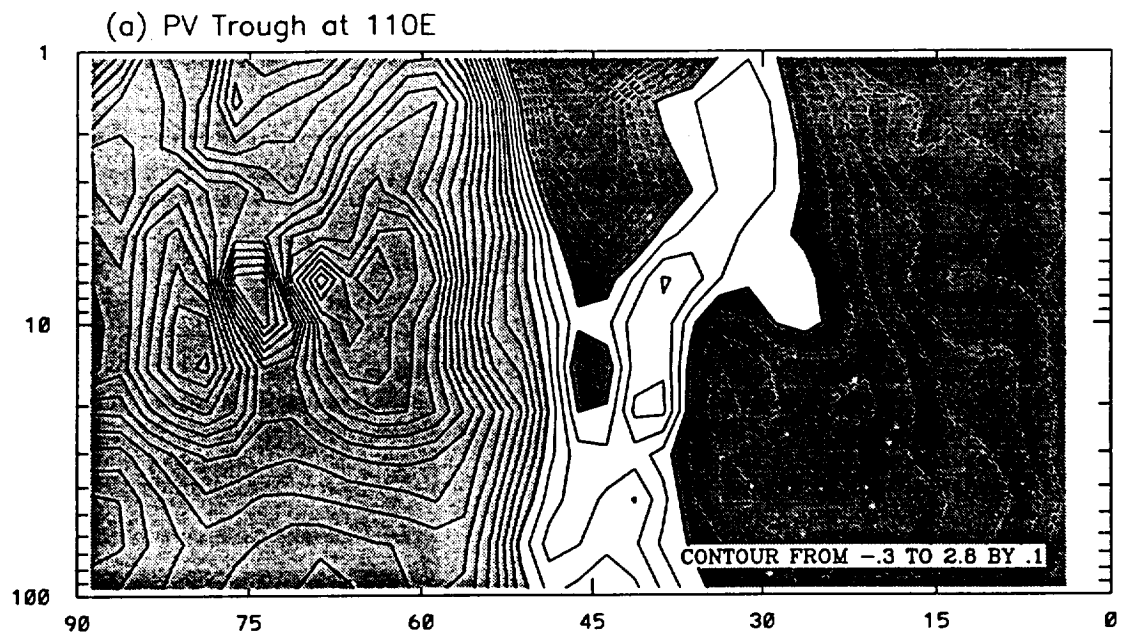


Fig. 2

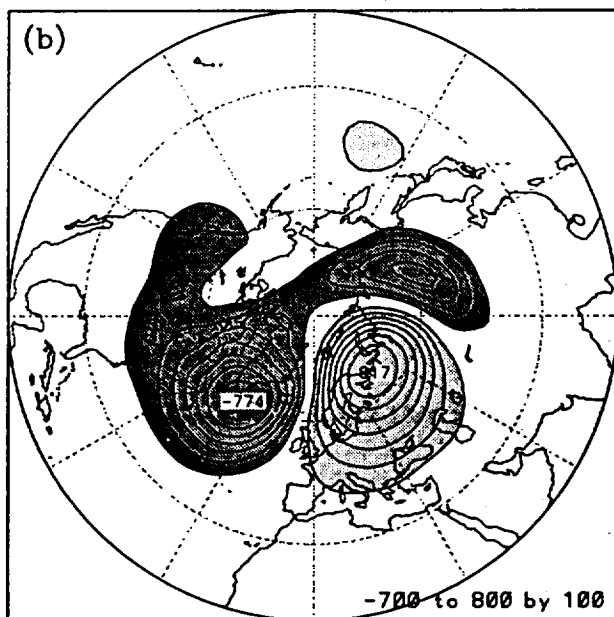
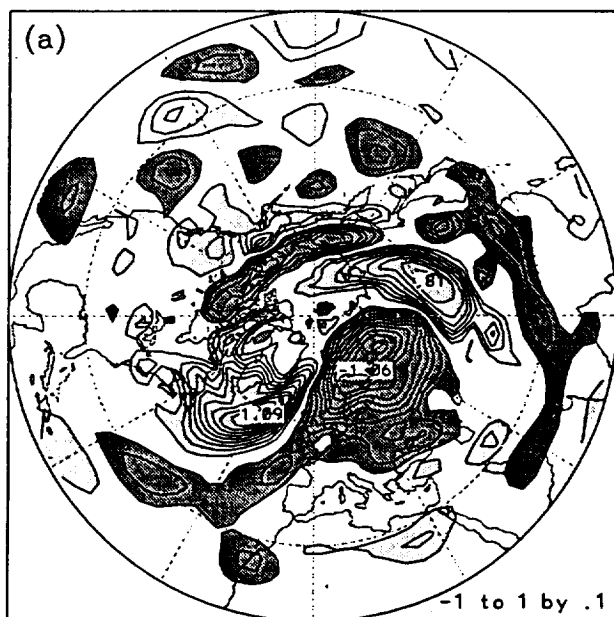


Fig. 3

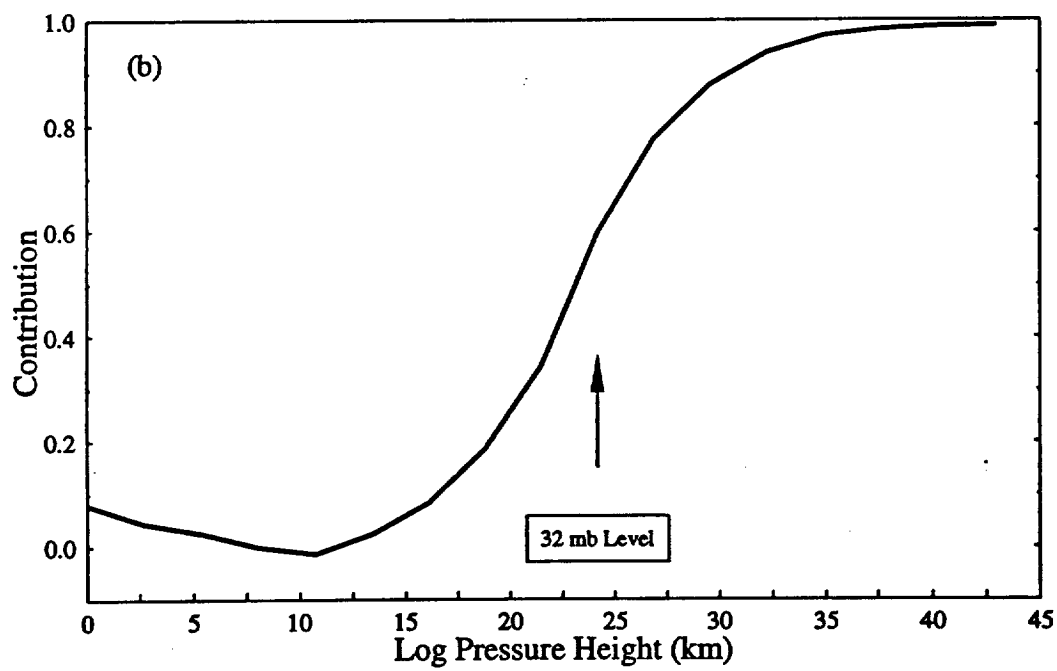
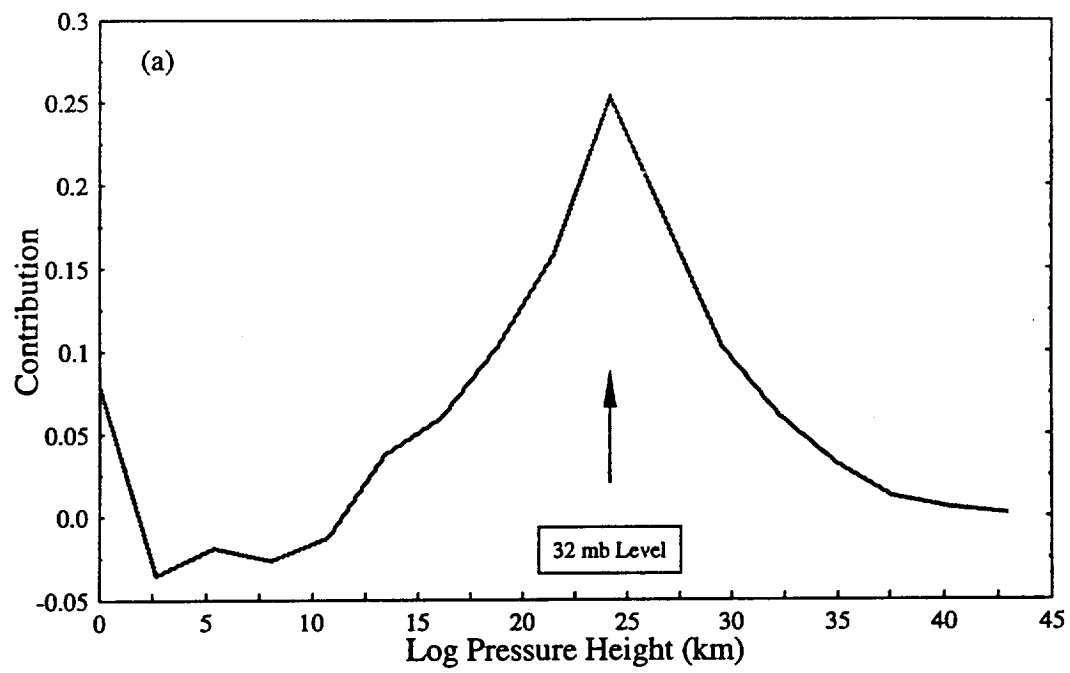


Fig. 4

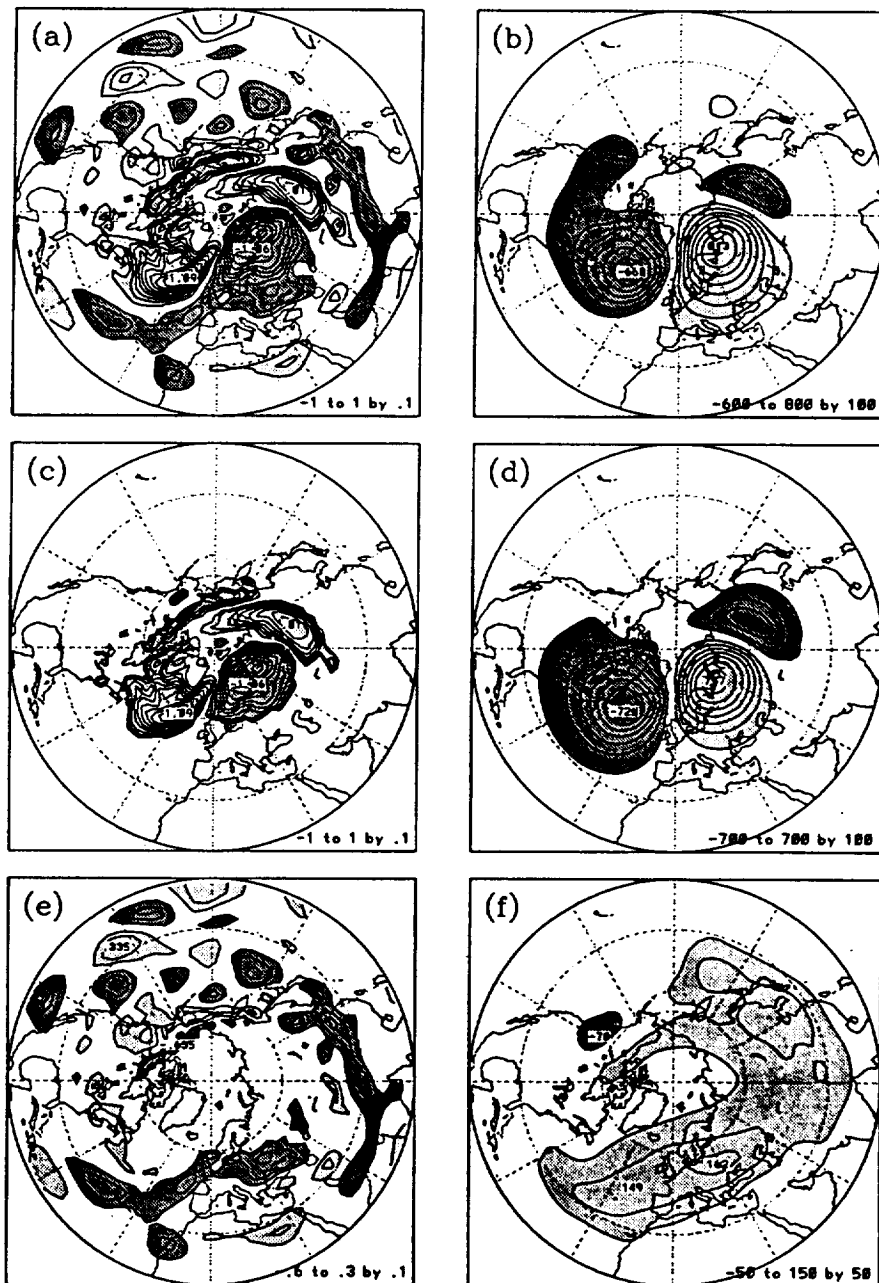


Fig. 5

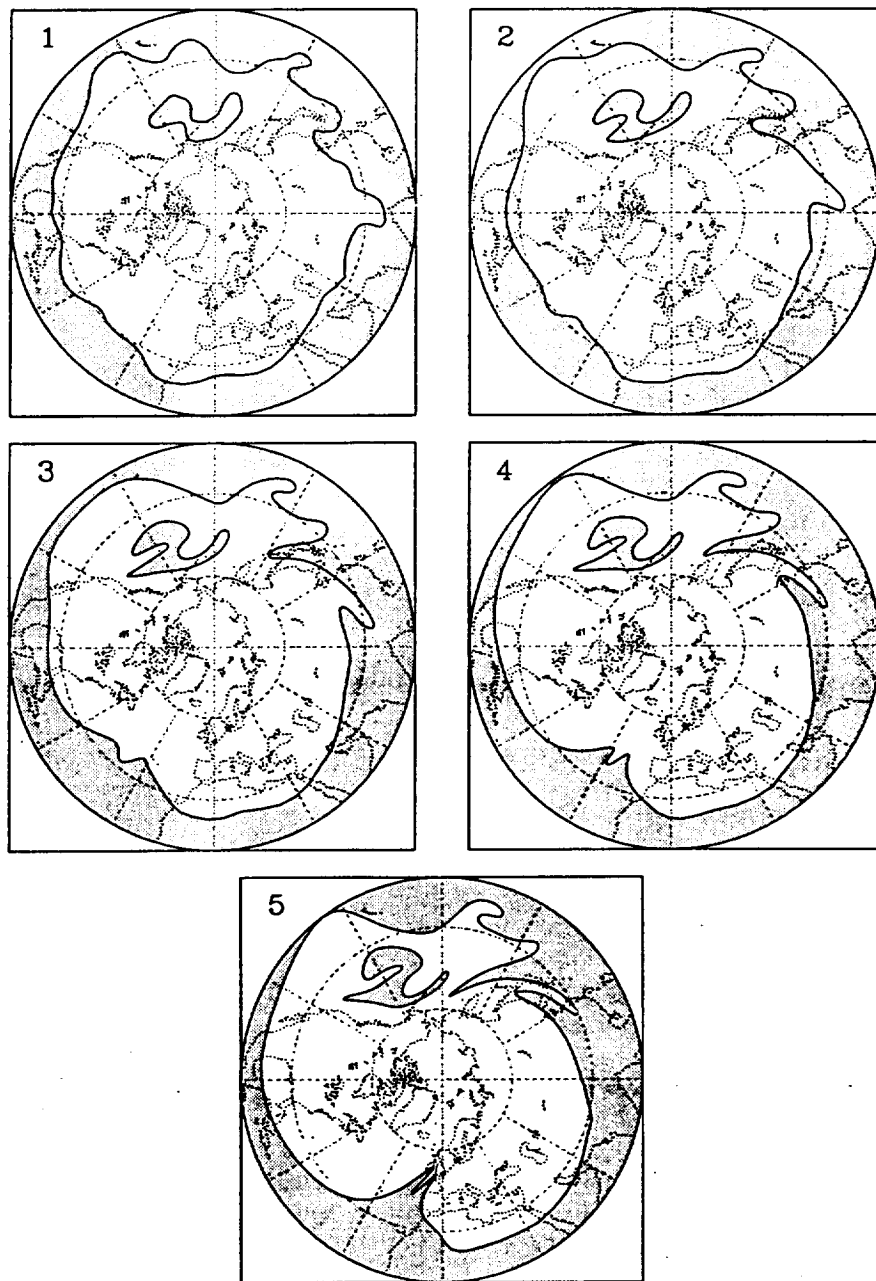


Fig. 6

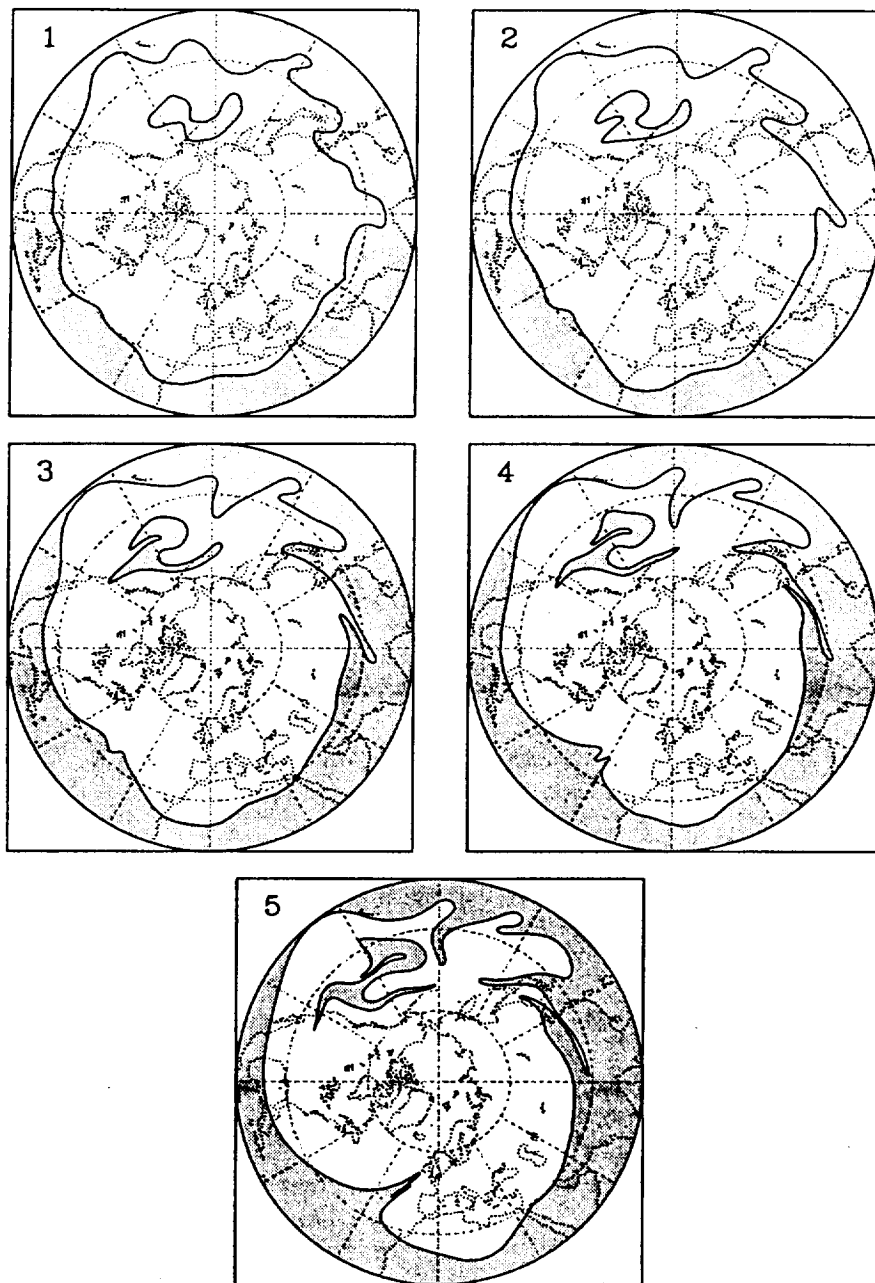


Fig. 7

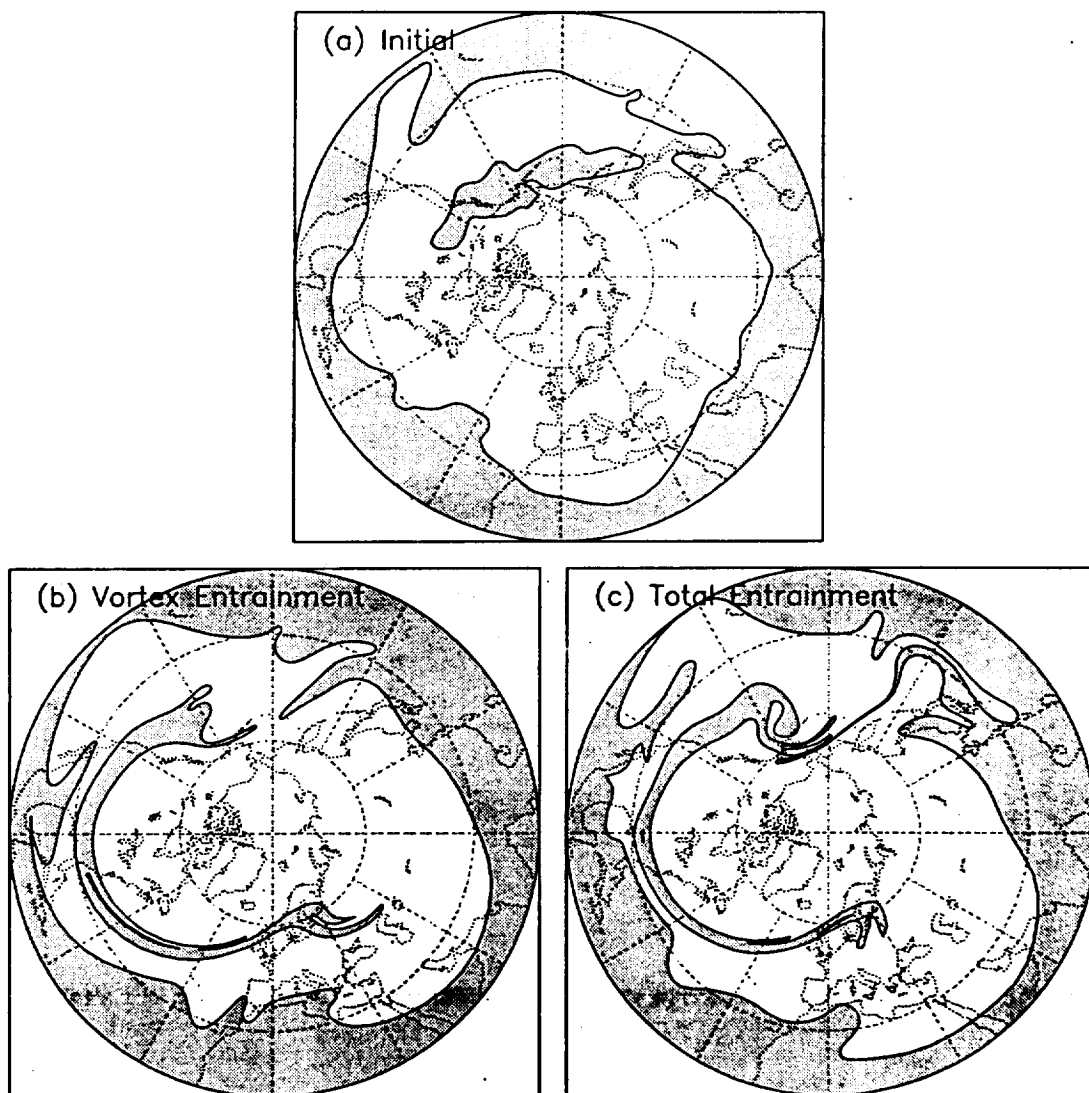


Fig. 8

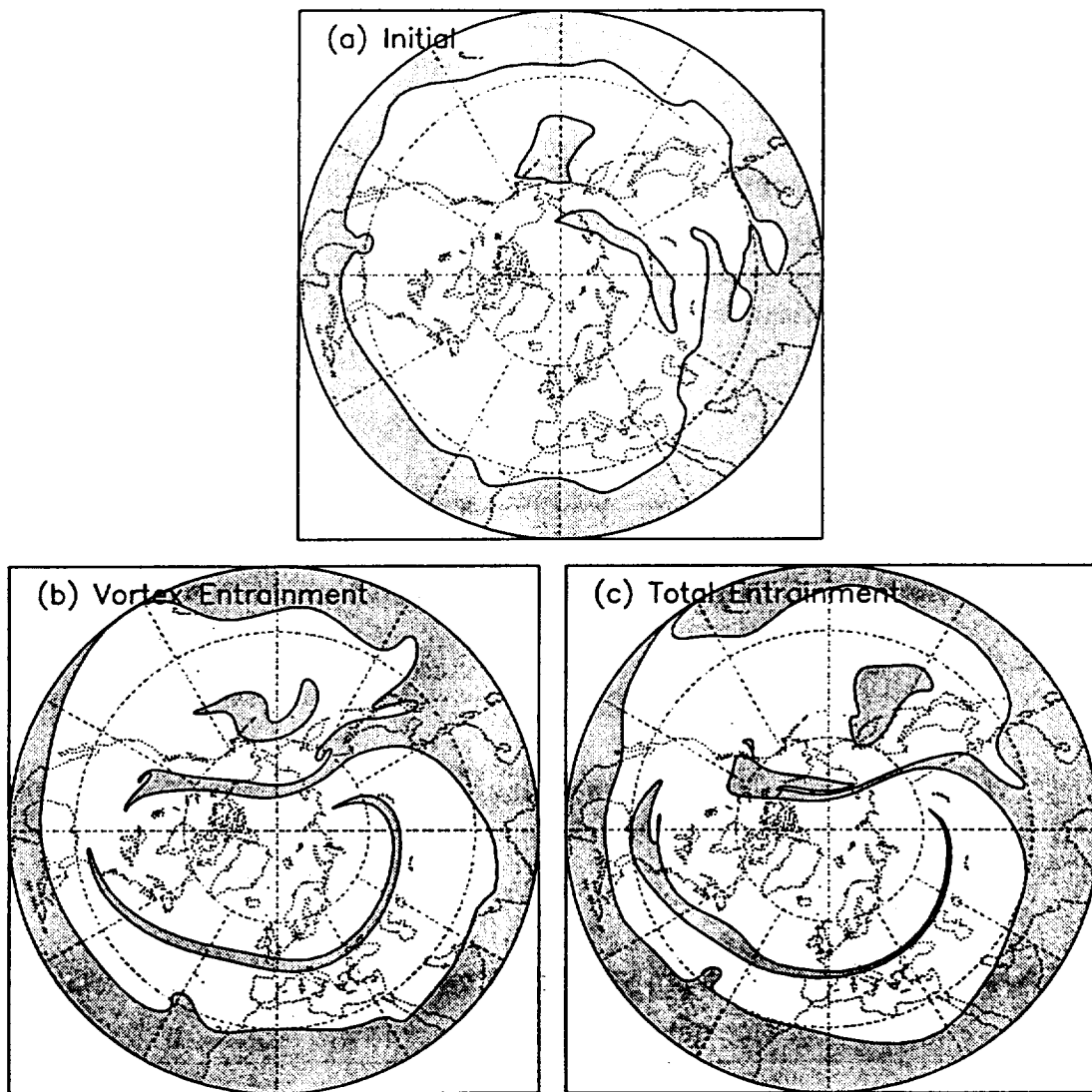


Fig. 9

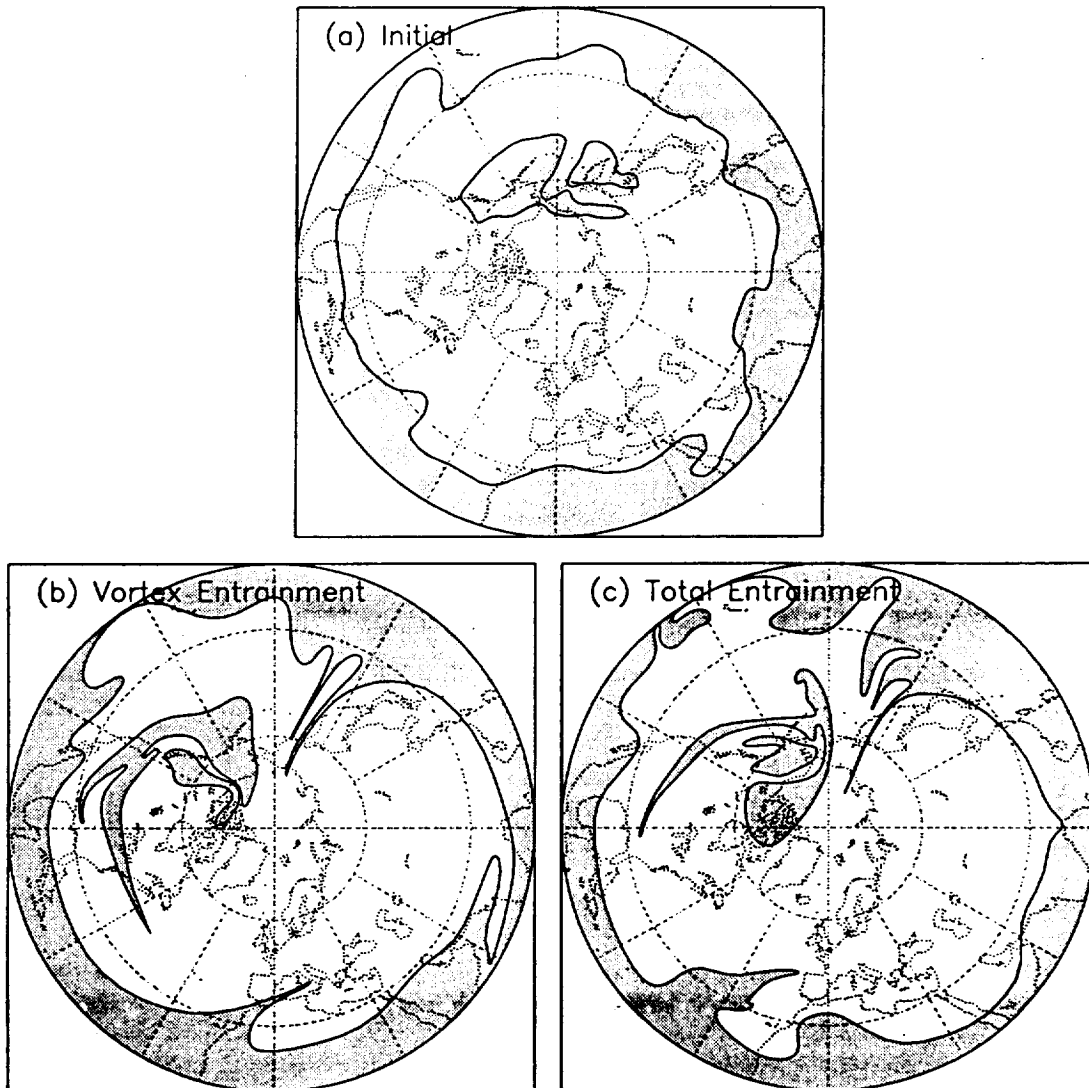


Fig. 10

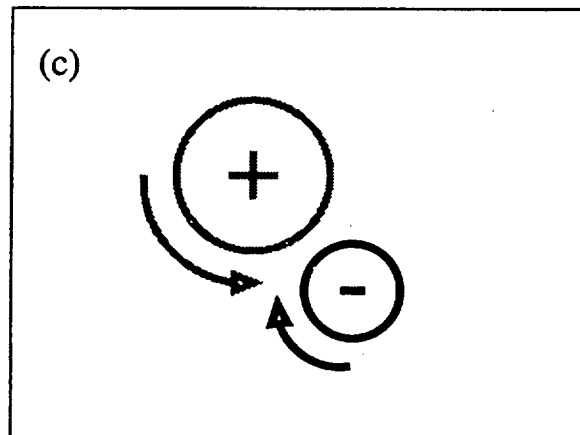
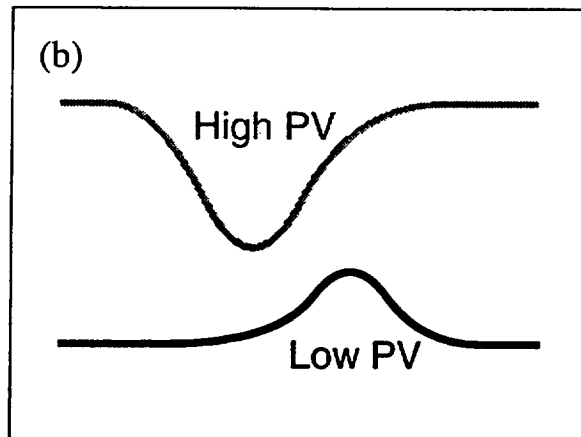
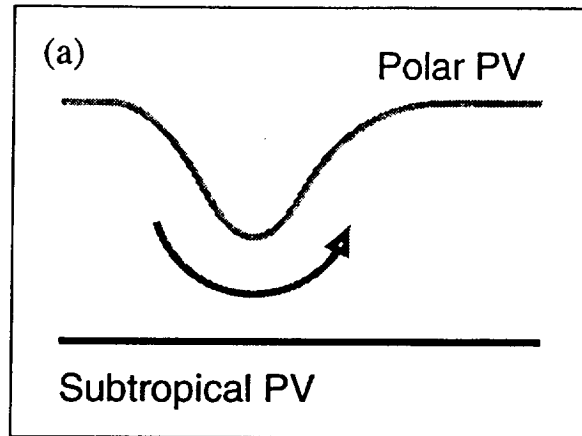


Fig. 11

# **A new perspective on the dynamical link between the stratosphere and troposphere**

Dana E. Hartley, Jose T. Villarín, Robert X. Black  
& Christopher A. Davis

# A new perspective on the dynamical link between the stratosphere and troposphere

Dana E. Hartley\*, Jose T. Villarin\*, Robert X. Black\* & Christopher A. Davis†

\* Georgia Institute of Technology, Atlanta, Georgia 30332-0340, USA

† National Center for Atmospheric Research, P.O. Box 3000, Boulder, Colorado 80307, USA

Atmospheric processes of tropospheric origin can perturb the stratosphere, but direct feedback in the opposite direction is usually assumed to be negligible, despite the troposphere's sensitivity to changes in the release of wave activity into the stratosphere<sup>1–3</sup>. Here, however, we present evidence that such a feedback exists and can be significant. We find that if the wintertime Arctic polar stratospheric vortex is distorted, either by waves propagating upward from the troposphere<sup>4</sup> or by eastward-travelling stratospheric waves<sup>5,6</sup>, then there is a concomitant redistribution of stratospheric potential vorticity which induces perturbations in key meteorological fields in the upper troposphere. The feedback is large despite the much greater mass of the troposphere: it can account for up to half of the geopotential height anomaly at the tropopause. Although the relative strength of the feedback is partly due to a cancellation<sup>7</sup> between contributions to these anomalies from lower altitudes, our results imply that stratospheric dynamics and its feedback on the troposphere are more significant for climate modelling and data assimilation than was previously assumed.

To test for feedbacks from the stratosphere on the troposphere, we use a method known as piecewise potential–vorticity (PV) inversion. PV inversion more generally means the deduction of geopotential anomaly fields (and related fields such as the wind field) from fields of PV anomalies in the atmosphere and potential temperature anomalies at the Earth's surface. The inversion process requires solving a Poisson-like equation, which indicates that the non-local effects are qualitatively similar to the induction of an electric field by electric charge<sup>8,9</sup>. It is a useful aid to understanding

atmospheric motions in circumstances where PV evolution is easily characterized. Piecewise PV inversion uses the superposition principle to calculate contributions to the geopotential height anomaly  $Z'$  attributable to PV anomalies in certain locations only<sup>10</sup>, analogous to calculating the electric fields that are due to only a subset of the total charge distribution.

The superposition principle is linear when the inversion is done on the basis of quasi-geostrophy (QG), and we accordingly use quasi-geostrophic PV<sup>11,12</sup> (hereafter, simply PV) throughout this study. Quasi-geostrophy is based on the assumption that the magnitude of horizontal wind acceleration is smaller than the force due to the Earth's rotation (small Rossby number) and that the vertical stability is approximately uniform along a pressure-altitude. In QG, PV anomalies,  $q'$ , and geopotential height anomalies,  $Z'$ , are linearly related by

$$q' = \mathcal{L}(Z') \quad (1)$$

where  $\mathcal{L}$  is a linear laplacian-type operator<sup>8</sup>. The linearity of equation (1) allows piecewise PV inversions to be performed unambiguously, as one can linearly superpose the contributions of individual PV anomaly 'pieces' to obtain the total  $Z'$  field.

Piecewise PV inversions have been applied in separate studies of tropospheric cyclogenesis<sup>10,13</sup> and the stratospheric polar vortex<sup>11</sup>. The latter research, which focused on how the stratospheric and mesospheric  $Z'$  fields are determined, included an exploratory analysis, using no tropospheric data, of the impact of two large stratospheric vortex deformations on the troposphere. Here we present an analysis and quantification of the influence of stratospheric PV anomalies relative to tropospheric PV anomalies in determining  $Z'$  in the upper troposphere. (The tropospheric PV anomalies include anomalies at the tropopause level: that is, those along the boundary between the troposphere and stratosphere.) Our study uses meteorological data for the winter of 1992/93 (analysed fields from the United Kingdom Meteorological Office, UKMO<sup>14</sup>) for both the troposphere and stratosphere, and diagnoses a broad range of cases of stratospheric polar vortex distortions, which are often associated with dramatic advective rearrangements of PV and ozone<sup>15,16</sup>. The radiative effects of carbon dioxide, ozone and other greenhouse gases in the stratosphere, along with the breaking of planetary-scale Rossby waves, are responsible for the strong winds and horizontal PV gradients observed at the edge of the vortex<sup>17,18</sup> which, when disturbed, can easily lead to strong advection. Stratospheric vortex distortions can be due to both the vertical propagation of planetary-scale Rossby waves from the

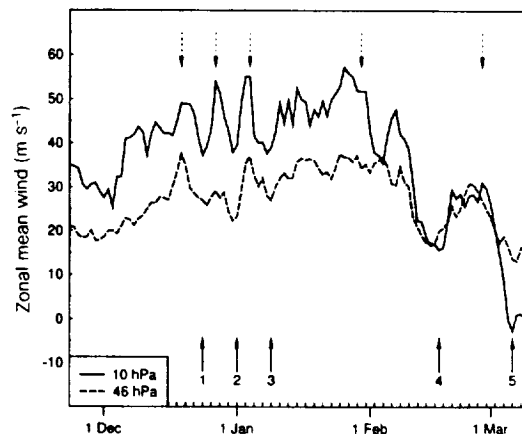


**Figure 1** Time series of the zonal mean wind at 61.25° N for the winter of 1992/93. The solid line is for 10 hPa (~30 km) and the dashed line is for 46 hPa (~20 km). Up-arrows mark vortex disturbance events and down-arrows mark non-events. The events are numbered for reference in the text and other figures.

Polar vortex disturbances are associated with significant decreases in the zonal mean wind near the edge of the stratospheric polar vortex. Figure 1 shows a time series of this quantity at 61.25° N for the winter of 1992–93. If we define an ‘event’ as a drop in wind speed of at least 10 m s<sup>-1</sup> at 10 hPa (~30 km) with a corresponding change at 46 hPa (~20 km), about five events occurred during this winter. ‘Non-events’ are defined as the times of maximum wind speeds between events (see Fig. 1). The PV distribution at 10 hPa for the wintertime average and for event 2 (January 1) are shown in Figs 2a and b, respectively. Figure 2c illustrates the vertical extent of the vortex distortion.

We first discuss the piecewise inversion for event 2. Figure 3 shows  $Z'$  at the tropopause during the event day. Figure 3b is the component of the tropopause  $Z'$  that is induced by PV anomalies located within the troposphere. It is clear that a large fraction of the  $Z'$  field is unaccounted for by tropospheric PV anomalies alone. The difference is due to the stratospheric influence shown in Fig. 3c. This component has magnitudes comparable to the  $Z'$  field induced by the tropospheric PV anomalies, indicating the large influence of stratospheric PV rearrangements on tropospheric dynamic fields.

To ascertain the location of the stratospheric PV anomalies that have the largest impact on tropospheric dynamical fields, we make use of a geopotential contribution function<sup>11</sup>. This measures the fraction of  $Z'$  at the tropopause that is due to the integrated effect of

PV anomalies above a specified altitude. This is calculated by taking the covariance of the observed tropopause  $Z'$  with the tropopause  $Z'$  induced by PV anomalies above the specified altitude. It is then integrated horizontally and normalized to give a fractional contribution. Figure 4a shows the geopotential contribution function as a function of altitude for each of the five events. On average, 34% of the tropopause  $Z'$  is induced by stratospheric PV anomalies, with most of this contribution from the lower (~12–16 km) and middle (~17–24 km) stratosphere and nearly negligible amounts from the upper stratosphere (~25–50 km).

The correspondence between the strength of the zonal mean wind change (Fig. 1) and the stratospheric contribution to the tropopause  $Z'$  is evident from Fig. 4. The two largest events (4 and 5) show the strongest stratospheric contribution to tropopause  $Z'$ . In fact, during event 5 stratospheric PV anomalies account for more than half of the tropopause  $Z'$ . We also note that the contributions of  $\theta'$  at the Earth's surface largely cancel the mid-tropospheric influence on tropopause  $Z'$ . This cancellation is evident in the contribution function, which exhibits a cancellation point at 7 km. In Fig. 4b, we plot the same contribution function for five non-events. For these cases, we find that, on average, about 15% of the tropopause  $Z'$  is induced by stratospheric PV anomalies. It is evident that the rearrangement of PV that occurs during vortex distortions induces strong geopotential height anomalies at the tropopause.

These results clearly indicate that stratospheric processes induce significant anomalies in dynamical fields at the tropopause. Although a coarsely resolved stratosphere is included in many current general circulation models and data assimilation systems used for tropospheric applications, our results suggest that a more realistic representation of the stratosphere may be required to enable such a model to properly simulate the troposphere. For upward-propagating linear Rossby waves, a suitable boundary condition at the tropopause may be sufficient to describe this feedback. But for internal stratospheric distortions and nonlinear breaking of vertically propagating Rossby waves, an atmospheric model must adequately represent the stratospheric processes in order to properly simulate the feedback on the troposphere. The feedback discussed here could significantly affect short-term and large-scale variations in the output from model simulations and data assimilations.

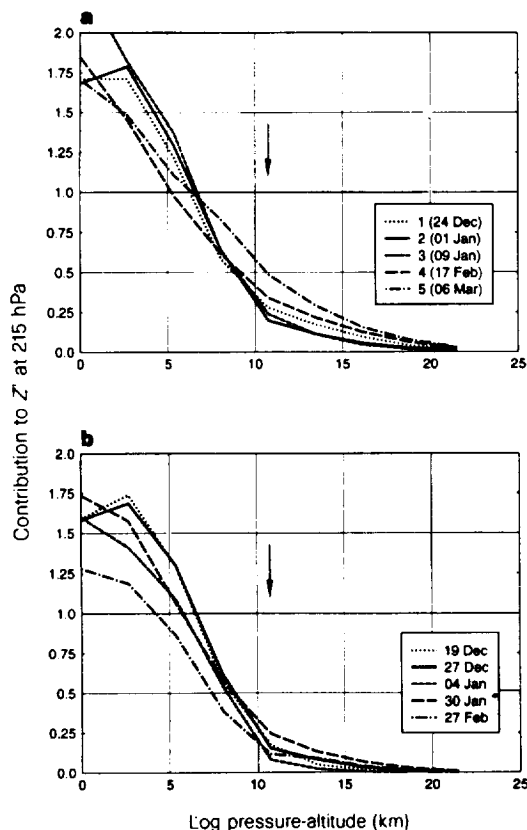


**Figure 4** Geopotential contribution function as a function of log pressure-altitude for (a) events and (b) non-events. The geopotential contribution function is the normalized covariance of the observed  $Z'$  at the tropopause (215 hPa) with  $Z'$  induced by PV anomalies ( $q'$ ) located above a specified pressure-altitude. This is a measure of the fraction of the Northern Hemisphere tropopause  $Z'$  that is induced by PV anomalies above a specific pressure-altitude. Log pressure-altitude ( $z^*$ ) is calculated from the UARS pressure levels by  $z^* = -H \ln(p/p_0)$ , where  $H = 7$  km and  $p_0 = 1,000$  hPa. The legends specify the date and event number that each line represents. An up-arrow is located at the log pressure-altitude of the tropopause. If the surface-induced  $Z'$  was included at  $z^* = 0$ , the contribution function at  $z^* = 0$  would be identically 1.0.

Received 14 October 1996; accepted 7 October 1997.

1. Boville, B. A. The influence of the polar night jet on the tropospheric circulation in a GCM. *J. Atmos. Sci.* **41**, 1132–1142 (1984).
2. Haigh, J. D. The impact of solar variability on climate. *Science* **272**, 981–984 (1996).
3. Kodera, K. & Chiba, M. Tropospheric circulation changes associated with stratospheric sudden warmings: A case study. *J. Geophys. Res.* **100**, 11055–11068 (1995).
4. Robinson, W. Irreversible wave-mean flow interactions in a mechanistic model of the stratosphere. *J. Atmos. Sci.* **45**, 3413–3430 (1988).
5. O'Neill, A. & Pope, V. Simulations of linear and nonlinear disturbances in the stratosphere. *Q. J. R. Meteorol. Soc.* **114**, 1063–1110 (1988).
6. O'Neill, A., Grose, W., Pope, V., MacLean, H. & Swinbank, R. Evolution of the stratosphere during Northern Winter 1991/92 as diagnosed from U.K. Meteorological Office Analyses. *J. Atmos. Sci.* **51**, 2800–2817 (1994).
7. Hoskins, B., McIntyre, M. & Robertson, A. Reply to Comment on 'On the use and significance of isentropic potential vorticity maps'. *Q. J. R. Meteorol. Soc.* **113**, 402–404 (1987).
8. Hoskins, B., McIntyre, M. & Robertson, A. On the use and significance of isentropic potential vorticity maps. *Q. J. R. Meteorol. Soc.* **111**, 877–946 (1985).
9. Bishop, C. & Thorpe, A. Potential vorticity and the electrostatics analogy: Quasi-geostrophic theory. *Q. J. R. Meteorol. Soc.* **120**, 713–731 (1994).
10. Davis, C. Piecewise potential vorticity inversion. *J. Atmos. Sci.* **49**, 1397–1411 (1992).
11. Robinson, W. Analysis of LIMS data by potential vorticity inversion. *J. Atmos. Sci.* **45**, 2319–2342 (1988).
12. Boville, B. A. The validity of the geostrophic approximation in the winter stratosphere and troposphere. *J. Atmos. Sci.* **44**, 443–457 (1987).
13. Davis, C. & Emanuel, K. Potential vorticity diagnostics of cyclogenesis. *Mon. Weath. Rev.* **119**, 1929–1953 (1991).
14. Swinbank, R. & O'Neill, A. A stratosphere–troposphere data assimilation system. *Mon. Weath. Rev.* **122**, 686–702 (1994).
15. Randel, W. J. et al. Stratospheric transport from the tropics to middle latitudes by planetary-wave mixing. *Nature* **365**, 533–535 (1993).
16. Waugh, D. W. Subtropical stratospheric mixing linked to disturbances in the polar vortices. *Nature* **365**, 535–537 (1993).
17. McIntyre, M. E. & Palmer, T. N. The ‘surf zone’ in the stratosphere. *J. Atmos. Terr. Phys.* **46**, 825–849 (1984).
18. Legras, B. & Dritschel, D. Vortex stripping and the generation of high vorticity gradients in two-dimensional flows. *Appl. Sci. Res.* **51**, 445–455 (1993).